Polymers **2014**, *6*, 1999-2017; doi:10.3390/polym6071999

OPEN ACCESS

polymers

ISSN 2073-4360

www.mdpi.com/journal/polymers

Article

Lipid Monolayers with Adsorbed Oppositely Charged Polyelectrolytes: Influence of Reduced Charge Densities

Thomas Ortmann [1], Heiko Ahrens [1], Sven Milewski [1], Frank Lawrenz [1], Andreas Gröning [1], André Laschewsky [2,3], Sebastien Garnier [3] and Christiane A. Helm [1,*]

[1] Institut für Physik, Ernst-Moritz-Arndt Universität, Felix-Hausdorff-Straße 6, D-17487 Greifswald, Germany; E-Mails: ortmann@uni-greifswald.de (T.O.); ahrensh@uni-greifswald.de (H.A.); sven.milewski@gmx.de (S.M.); lawrenz@uni-greifswald.de (F.L.); groening@physik.uni-greifswald.de (A.G.)

[2] Fraunhofer Institute for Applied Polymer Research, Geiselberg Str. 67, D-14476 Potsdam-Golm, Germany; E-Mail: andre.laschewsky@iap.fraunhofer.de

[3] Institut für Chemie, Universität Potsdam, Karl-Liebknecht-Str. 24-25, D-14476 Potsdam-Golm, Germany; E-Mail: sebastien.garnier@basf.com

* Author to whom correspondence should be addressed; E-Mail: helm@uni-greifswald.de; Tel.: +49-(0)3834-86-4710; Fax: +49-(0)3834-86-4712.

Received: 30 April 2014; in revised form: 26 June 2014 / Accepted: 27 June 2014 / Published: 10 July 2014

Abstract: Polyelectrolytes in dilute solutions (0.01 mmol/L) adsorb in a two-dimensional lamellar phase to oppositely charged lipid monolayers at the air/water interface. The interchain separation is monitored by Grazing Incidence X-ray Diffraction. On monolayer compression, the interchain separation decreases to a factor of two. To investigate the influence of the electrostatic interaction, either the line charge density of the polymer is reduced (a statistic copolymer with 90% and 50% charged monomers) or mixtures between charged and uncharged lipids are used (dipalmitoylphosphatidylcholine (DPPC)/ dioctadecyldimethylammonium bromide (DODAB)) On decrease of the surface charge density, the interchain separation increases, while on decrease of the linear charge density, the interchain separation decreases. The ratio between charged monomers and charged lipid molecules is fairly constant; it decreases up to 30% when the lipids are in the fluid phase. With decreasing surface charge or linear charge density, the correlation length of the lamellar order decreases.

Keywords: lipid monolayer; polyelectrolyte adsorption; statistical copolymer; two-dimensional phases; surface charge; nematic phase; grazing incidence X-ray diffraction

1. Introduction

Traditional Langmuir monolayers at the air/water interface are formed from amphiphilic, mostly lipid-like molecules. They contain hydrophilic heads that anchor onto the water subphase and hydrophobic tails that point toward the air. These monolayers have gained interest in the field of chemistry, physics and life science [1–4]. They serve, e.g., as cell membrane mimics or as model systems for studying two-dimensional (2-D) phase transitions and ordering. An advantage is the adjustable surface charge, as well as the accessibility to many different characterization techniques. Thus, the surface coverage and conformation of adsorbed macromolecules (proteins, DNA or nanoparticles) has been investigated [5–7]. The binding of the macromolecules affects the interactions between the lipid head-groups, and thus the phases and phase transitions of the lipid monolayer [8].

Most water-soluble polymers are charged, *i.e.*, they are polyelectrolytes (PEs). They adsorb onto oppositely charged surfaces. If linear PEs are adsorbed from salt-free solutions, the electrostatic interaction between the charges along the chain has a large amplitude and is long-ranged. Therefore, the PEs adsorb in a flat conformation [9,10]. The surface coverage increases on increase of the PE concentration in the solution until saturation is reached [11]. At maximum PE coverage, the surface charge of the substrate is reversed. However, at low PE concentration in solution, the surface coverage is low. Then, the adsorbed PEs do not compensate the surface charge of the substrate. The adsorbed chains repel each other electrostatically. Therefore, they adsorb in a lamellar manner [12–14] According to theoretical calculations [15,16], a condition of the two-dimensional lamellar phase is that no charge reversal occurs.

This description is very qualitative. One cannot predict, when flatly adsorbed PEs are in a disordered or in a lamellar conformation [15,16]. It is clear that surface charge, and the chain stiffness (measured by the persistence length) are important parameters. However, there are few experiments which describe the two-dimensional lamellar phase, namely references [12–14]. Suitable model systems are PEs adsorbed to a lipid monolayer or bilayer, as the few publications on the subject show. An Atomic Force Microscopy (AFM) study of polystyrene sulfonate (PSS) adsorbed to a model membrane on a solid substrate [12] studies very weakly charged surfaces. Lipid monolayers at the air/water interface are studied by X-ray techniques [13,14]. In the two-dimensional lamellar phase, the interchain separation can be determined by Grazing Incidence Diffraction (GID). On monolayer compression, the surface charge and also the separation of the PE chains is reduced by a factor of two (Scheme 1) [13,14].

Scheme 1. Side view of the monolayer with adsorbed polyelectrolyte (PE) at the air-water interface (**a**) along the PE chain and (**b**) perpendicular to the PE chains. Additionally, on the right, the increase of the chain separation, which occurs when the area per lipid molecule is decreased, is schemed out.

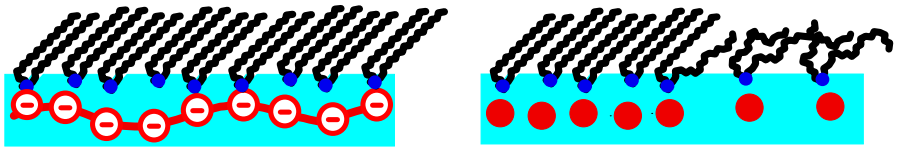

(**a**) (**b**)

Recently, we investigated polystyrene sulfonate (PSS) in a lamellar phase adsorbed onto an oppositely charged lipid monolayer. The lipids were dioctadecyldimethylammonium (DODA) with a positively charged head group [14]. PSS is a strong polyanion, therefore, in these experiments, the electrostatic force is very large [5,17,18]. We varied the molecular weight of PSS. We found that in the lamellar phase the surface coverage and the interchain separation are not influenced by the molecular weight of the PEs (exception: very low molecular weight PEs and very low surface charge in the LE phase of the lipids). An increase of the surface charge density occurs when the lipid monolayer is compressed. If the monolayer shows both a liquid expanded (LE) and a liquid condensed (LC) phase, the area per lipid molecule is reduced by a factor of two [1,2]. Simultaneously, the surface charge density of the monolayer increases by a factor of two. The adsorbed PEs influence the interactions between the lipid molecules, which can best be investigated by exploring the LE/LC phase transition [18–20] PEs in salt-free solution have a much larger persistence length than neutral polymers [21]. If the contour length L_K is smaller than the persistence length L_P ($L_K \leq L_P$) then the polymer is approximated as an elastic rod. Only if the contour length exceeds the persistence length ($L_K \geq L_P$), then the chain can be described as a flexible polymer.

The lateral pressure π_c, which marks the LE/LC phase transition of lipid monolayers, does depend very strongly on the molecular weight. In the past, a reduction of the transition pressure π_c due to decreased electrostatic repulsion between the lipid head groups has been observed [22]. The surface coverage of the PSS is independent of its molecular weight. However, a reduction of π_c with the molecular weight of PSS has been observed. It cannot be attributed to electrostatic forces as described by the DLVO theory [18,19]. π_c decreases on increase of the molecular weight, until the contour length corresponds to the persistence length, then π_c is independent of the molecular weight. For polystyrene sulfonate (PSS) a persistence length of L_P = 210 Å was found (molecular weight 16 kDa) [14] which is an order of magnitude larger than the persistence length of neutral polymers ($L_{P,steric}$ = 30 Å) [23]. It suggests an effective ion concentration at the monolayer/polyelectrolyte interface of 10 mmol/L, even though the ion concentration in solution is two to three orders of magnitude smaller (≈0.01 mmol/L). Concomitant with the decrease of the transition pressure π_c, the temperature dependence of the transition enthalpy ΔH weakens until the contour length L_K exceeds the persistence length L_P. Then the temperature dependence of the phase transition enthalpy is low and constant. The lipids in the LE phase are partially immobilized by binding to a flexible rod; they loose entropy in the LE phase. The longer the flexible rod, the lower are transition pressure und transition enthalpy. If $L_K \geq L_P$, polymer length is no longer important.

Now, we want to decrease the influence of the electrostatic forces. We use two different approaches. First, the line charge density of the PE is reduced (see Scheme 2). The fraction of charged monomers in a statistical copolymer is 90% and 50%. Second, the surface charge density is reduced by mixing cationic dioctadecyldimethylammonium bromide (DODAB) with a zwitterionic lipid dipalmitoylphosphatidylcholine (DPPC).

Scheme 2. Polyelectrolytes adsorbed to oppositely charged monolayers: (**a**) strong polyanion polystyrene sulfonate (PSS) and (**b**) strong polyanion random copolymer P–TrisAA$_x$–rand–AMPS$_{1-x}$ (x = 0.1, 0.5).

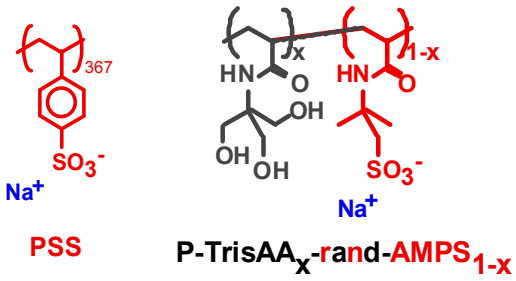

(**a**) (**b**)

We use PEs with large molecular weight, to actually adsorb a flexible polymer, and not an elastic rod. The PE concentration is low and leads to PE adsorption in a lamellar manner, 0.01 mmol/L with respect to the monomer concentration [12–14]. We use GID to measure the surface coverage of the PEs [24] due to its high resolution. X-ray reflectivity can resolve changes in the surface coverage within 15%–20% for one monolayer, for GID the resolution is better (a few percent). We want to explore subtle changes, and compare different polyelectrolytes and monolayers of different composition. With X-ray reflectivity, one can obtain an electron density profile. One has to assign a slab to the adsorbed polyelectrolyte layer. With the lipids used in this work, this slab contains besides the PE also the head group of the lipids. However, to obtain a quantitative surface coverage one has to make for each system assumptions. One needs to know the volume of a lipid head group and the volume of a PE monomer. One has to guess the degree of hydration of both monomer and lipid head group. Usually the number of water molecules within the head group slab is reduced on monomer compression [1,24]. Since we compare different polyelectrolytes and different lipid monolayers, we would have to make many assumptions. In contrast, with GID, the position of the X-ray diffraction peaks can be resolved within 1%. We think the surface coverage is correct within a few percent, since we see that film-to-film variation and film history (first or second compression, expansion, *etc.*) influence the position of the Bragg peaks [14], but we never explored these effects in detail.

2. Experimental Section

2.1. Materials

The cationic lipid dioctadecyldimethylammonium bromide (DODAB) and the zwitterionic DPPC are from Avanti, Alabaster, AL, USA. The strong polyanions are PSS sodium salt with molecular weight M_w = 16 and 75.6 kDa, respectively and with polydispersity index PDI ≤ 1.1 and degree of

sulfonation 97% (Polymer Standards Service, Mainz, Germany). The random copolymers are P–TrisAA$_x$–rand–AMPS$_{1-x}$ (x = 0.1, 0.5). The latter is made by "diluting" the permanently negatively charged monomer sodium 2-acrylamido-2-methylpropanesulfonate (AMPS) with the neutral monomer *N*-tris(methylol)methylacrylamide (TrisAA, see Scheme 2) via random radical copolymerization), following an established procedure [25] The molecular weight exceeds 50 kDa, the PDI is presumably rather large (>2).

2.2. Langmuir Trough and Isotherms

Surface pressure isotherms (π-A isotherms) are measured on a Teflon trough (Riegler and Kirstein, Potsdam, Germany). The surface pressure is recorded with a Wilhelmy-type pressure measuring system using filter paper as plate with an accuracy of 0.1 mN/m. The area of the trough is 3.0 × 30 cm^2. DODA or DODA/DPPC, respectively, is spread from 0.14 mmol/L chloroform/methanol (3:1) [volume] solutions, using a 100 µL syringe.

The monolayers are compressed at a rate of 3 Å^2/(molecule·min) after allowing 10 min for the evaporation of the solvent. Ultrapure water from a Milli-Q system with a resistance above 18 MΩ is used. Always, the subphase contains PE. The PE concentration is set to 0.01 mmol/L (with respect to the monomer concentration) and kept constant, leading to a pH value slightly below 6. The temperature is controlled by a thermostat (DC-30 Thermo-Haake, Haake-Technik, Karlsruhe, Germany). All isotherms shown are obtained during the first compression of the monolayer.

2.3. Grazing Incidence X-Ray Diffraction

Grazing-incidence diffraction measurements were performed at the Hamburger Synchrotron laboratory (HASYLAB) situated at the Deutsche Elektronen-Synchrotron (DESY, Hamburg, Germany). The liquid surface diffractometer at the undulator beam line BW1 was used [26]. With this technique, a monochromatic X-ray beam (λ = 1.303 Å) strikes the surface at grazing-incidence angle α_i = 0.85 α_c (α_c = 0.13° is the critical angle for total reflection). The intensity of the Bragg peaks is measured by a linear position sensitive detector (PSD) (Mythen detector, Dectris, Switzerland) as a function of the vertical scattering angle α_f [13,27]. The resolution of 0.09° of the in-plane scattering angle 2θ is given be the Soller collimator in front of the PSD.

According to the geometry of diffraction, the scattering vector $\boldsymbol{Q}$ has an in-plane component, $Q_{xy} = 2\pi/\lambda\left(\cos^2\alpha_i + \cos^2\alpha_f - 2\cos\alpha_i\cos\alpha_f\cos 2\theta\right)^{1/2}$ and an out-of-plane component $Q_z = 2\pi/\lambda\left(\sin\alpha_i + \sin\alpha_f\right)$. The positional correlation length ξ can be determined from the full width half maximum (f_{whm}). For an exponential decay of positional correlation as observed in liquid crystals, corresponding to a Lorentzian as a Bragg profile, one obtains $\xi = 2/f_{\mathrm{whm}}(Q_{xy})$.

The position-resolved scans were corrected for illuminated area. Model peaks are assumed to be Lorentzians in the in-plane direction and Gaussians in the out-of-plane direction, and are fitted to corrected intensities. The lattice spacing is obtained from the in-plane diffraction data.

3. Results and Discussion

3.1. Isotherms and Thermodynamics

Figure 1 shows a series of π-A isotherms of lipid monolayers with adsorbed P–TrisAA$_x$–rand–AMPS$_{1-x}$, for x = 0.1 and 0.5. Each isotherm has the typical shape known from fatty acid or phospholipid monolayers [1]. The fluid phase of the lipids is marked by an increase in surface pressure π_c on monolayer compression. A break in the slope at π_c marks the onset of the LE/LC phase transition. The isotherms show the typical plateau indicative of the coexistence of lipids in the LE and LC phase. π_c is determined by fitting two straight lines to the isotherm, one at the end of the LE phase and one at the beginning of the plateau region. π_c is assigned to the intersection. At the end of the coexistence region, the lipids are in the LC phase and π increases steeply.

Figure 1. Surface pressure—area isotherms of lipid monolayers on 0.01 mmol/L PE solution (with respect to the monomer concentration). (**a**,**b**): dioctadecyldimethylammonium (DODA) isotherms with the statistical copolymer P–TrisAA$_x$–rand–AMPS$_{1-x}$ at temperatures indicated. ((**a**) x = 0.9; (**b**) x = 0.5). The surface pressure π_c marks the onset of the LE/LC phase transition. The temperature dependence of π_c is shown in the insets. (**c**) π–A isotherms of DODA/DPPC mixtures at 20 °C with PSS (M_w = 77 kDa) in the subphase. The composition of the monolayer is varied. The inset shows the average area per molecule at 30 mN/m.

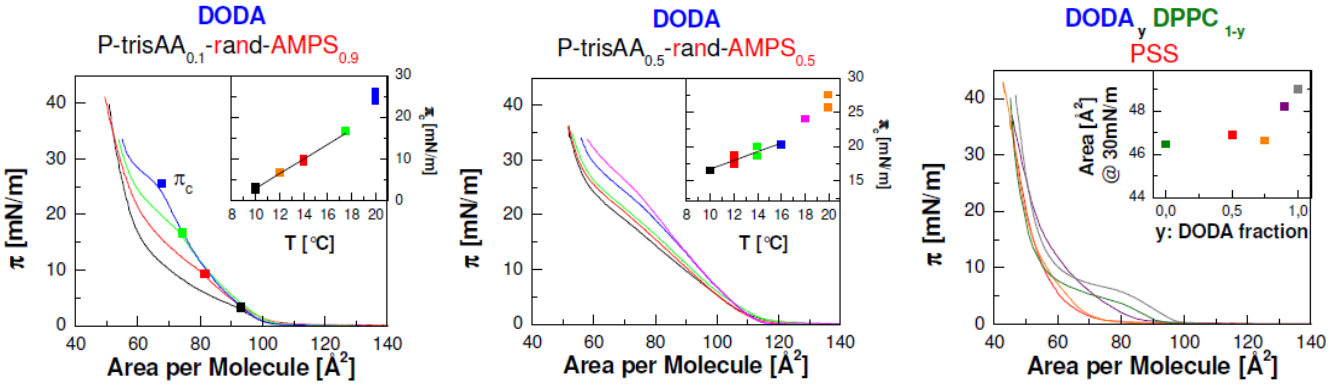

For each system the temperature is varied. As expected, the phase transition pressure π_c increases on heating. However, the temperature dependence of π_c depends on the composition of the statistical copolymer: if the charged monomers AMPS form 90% of the statistical copolymer, the temperature dependence is strong ($\partial\pi_c / \partial T$ = 1.76 mN/(m·K)). However, if the fraction of charged monomers is decreased to 50%, then the temperature dependence is decreased by more than a factor of two ($\partial\pi_c / \partial T$ = 0.68 mN/(m·K), see Table 1). Additionally, Figure 1 shows the isotherms of DODA/DPPC mixtures with PSS in the subphase. If the lipid monolayer consists of either pure DODA or pure DPPC, the isotherms show a clear LE/LC phase transition. When the monolayer consists of 90% or 75% DODA, the pressure increases at 90 Å^2/molecule, suggesting some fluid lipids. However, the decrease of the transition pressure π_c is attributed to the changed head group interactions of the mixed lipid monolayer. Note that DODA, DPPC and dipamitoylphosphatidylehtanolamine (DPPE) have the

same saturated alkyl tails with 16 C-atoms (note that for DODA two C-atoms of each hydrocarbon chain are attributed to the head group). DPPE shows no fluid phase at 20 °C [1,28]. Therefore, the in-plane attraction of the alkyl tails is strong. However, DODA and DPPC show a clear LE/LC phase transition. Therefore, one has to introduce an additional repulsion between the lipids which is attributed to the head group interaction. In the case of DODA, the liquefying effect is due to electrostatic head group repulsion [13,24]. For DPPC, the repulsion is due to the bulky head groups whose space requirements introduce an additional repulsive force between the lipid molecules. The head-groups of DPPC are zwitter-ionic; they do not repel each other electrostatically [1,29].

The repulsion between the head groups of DODA and DPPC have different physical origins. Therefore, mixing the two lipids reduces both the DODA–DODA and DPPC–DPPC repulsion. In the LC phase, the average distance between the charged DODA head groups is increased compared to a pure DODA monolayer. Therefore, the electrostatic repulsion of the DODA head groups is reduced.

Table 1. The temperature dependence of the phase transition pressure $d\pi_c / dT$ of DODA monolayers as function of the adsorbed PE molecules. When polystyrene sulfonate (PSS) is adsorbed, $d\pi_c / dT$ decreases with the molecular weight of PSS by a factor of two, until M_w (PSS) = 16 kDa is reached (superscript "1" indicates data from [14]). The composition of the statistical copolymer P–TrisAA$_x$–rand–AMPS$_{1-x}$ influences $d\pi_c / dT$. The subphase concentration of all PEs is 0.01 mmol/L in monomer units.

DODA monolayer	$\frac{d\pi_c}{dT}$ (mN/(m·K))
PSS (4 kDa)[1]	1.58
PSS (6.5 kDa)[1]	1.28
PSS (8.6 kDa)[1]	1.04
PSS (16, 33, 77, 168, 1330 kDa)[1]	0.85 ± 0.05
P–trisAA$_{0.1}$–rand–AMPS$_{0.9}$	1.76
P–trisAA$_{0.5}$–rand–AMPS$_{0.5}$	0.68

Furthermore, the steric repulsion of the DPPC head-groups is decreased, due to the incorporation of small DODA head groups in the monolayer. The decreased head group repulsion solidifies the lipid monolayer, and the LE/LC phase transition pressure π_c of the lipid mixtures is reduced.

To better understand the LE/LC phase transition of the monolayers, the transition enthalpy ΔH is calculated according to the two-dimensional Clausius-Clapeyron equation:

$$\Delta H = \frac{\partial \pi_c}{\partial T} T (A_{fl} - A_s) N_A \quad (1)$$

T denotes the temperature and N_A the Avogradro constant. A_{fl} and A_s are the molecular areas in the fluid and gel phase, respectively. In Figure 2 the temperature dependence of ΔH of DODA monolayers with different adsorbed PEs is shown. The strongest temperature dependence is found with adsorbed statistical copolymer consisting of 90% charged AMPS, the weakest when the copolymer consists of 50% charged AMPS. DODA on pure water is in-between.

Figure 2. Transition Enthalpy ΔH of DODA monolayers on pure water (black) and with statistical copolymer P–trisAA$_x$–rand–AMPS$_{1-x}$ (x = 0.1 green, 0.5 red) in the subphase. The concentration of P–trisAA$_x$–rand–AMPS$_{1-x}$ is 0.01mmol/L in monomer units.

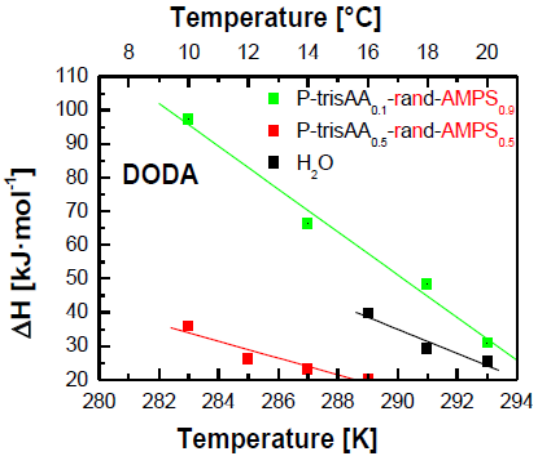

3.2. Lamellar Phase and Adsorbed PEs

Diffraction peaks: The lamellar phase of the adsorbed PSS is studied with grazing incidence diffraction measurements along the compression isotherm. A typical measurement for PSS (M_w = 16 kDa, L_K = 210 Å) adsorbed to a DODA monolayer is shown in Figure 3a. When the lipids are in the LE phase, a low-angle peak is observed. It is attributed to aligned PSS chains separated by a distance d_{PE}. On monolayer compression the low-angle peak shifts to larger Q_{xy} values (from 0.12 to 0.16 Å^{-1}), indicating a decrease of the interchain separation d_{PE}. In the coexistence region, the low-angle peak observed in the fluid phase exhibits a constant position [14]. Simultaneously, at larger Q_{xy}-values a peak with an unusual structured rod in Q_z-direction appears (two peaks at the same Q_{xy} and different Q_z positions). The positions of the two different low-angle peaks never coincide (no peaks for 0.181 Å^{-1} ≤ Q_{xy} ≤ 0.230 Å^{-1}) [14]. The structured rod arises from two scattering centers with the same periodicity, one is due to aligned PSS chains and the other to an induced corrugation of the film/air interface [13,27]. At the end of the coexistence region, high-angle peaks due the lipid structure can be resolved (see Figure 3). One peak occurs at low Q_z, the other broad peak at high Q_z is actually a superposition of two peaks, as detailed analysis shows. On monolayer compression, the wide angle peak positions shift to larger values in Q_{xy} direction, therefore the lattice distance of the alkyl tails decrease. Simultaneously, the peak positions in Q_z-direction decrease, *i.e.*, the tilt angle decreases. As shown previously, the alkyl tails of the DODA molecules have the same monoclinic tilted phase as on clean water [13].

The surface charge of the monolayer is reduced by mixing DODA with increasing proportions of DPPC, mixtures of 90%, 75% and 50% DODA are used. Small angle GID peaks due to aligned PSS chains are only observed, when the mixtures contain 90% or 75% DODA (see Figure 3). When the monolayers contain 50% DODA, no small angle peaks are found. For 90% and 75% DODA, the same features of the small angle peaks are observed as for pure DODA monolayers (one simple peaks for the LE phase, one peak with a structured rod for the LC phase). The large angle diffraction peaks caused by the lipid structure show a similar monoclinic tilted phase as for pure DODA monolayers.

When the DODA proportion is reduced to 75%, the onset of the surface pressure increase at 75 Å^2 suggests a LE phase. No clear LE/LC phase transition can be discerned. However, above 3–5 mN/m wide angle peaks are observed which indicate that at least some lipids are in the LC phase. These wide angle peaks are similar to those obtained with pure DODA monolayers, yet the peak at low Q_z shows a reduced width in Q_{xy} direction, indicative of an increased correlation length perpendicular to the tilt direction. Actually, a pure DPPC monolayer shows an orthorhombic lattice with a tilt towards the next neighbour, the corresponding diffraction pattern shows two peaks, one at Q_z = 0. The structure of $DODA_{0.5}DPPC_{0.5}$ is similar: it is orthorhombic with a tilt towards the next neighbor (data not shown).

Figure 3. Small and wide angle Grazing Incidence X-ray Diffraction (GID) measurements along $DODA_yDPPC_{1-y}$ isotherms at the molecular areas indicated (0.01 mmol/L PSS in monomer units and T = 20 °C). The low-angle diffraction peaks are due to aligned PSS chains, the wide-angle peaks measure the lipid structure. (**a**) pure DODA (M_w (PSS) = 16 kDa). (**b**) $DODA_{0.9}DPPC_{0.1}$ (M_w (PSS) = 76 kDa). (**c**) $DODA_{0.75}DPPC_{0.25}$ (M_w (PSS) = 76 kDa). For the small angle peaks, background is subtracted. Contour plots are calculated from least square fits to appropriate models.

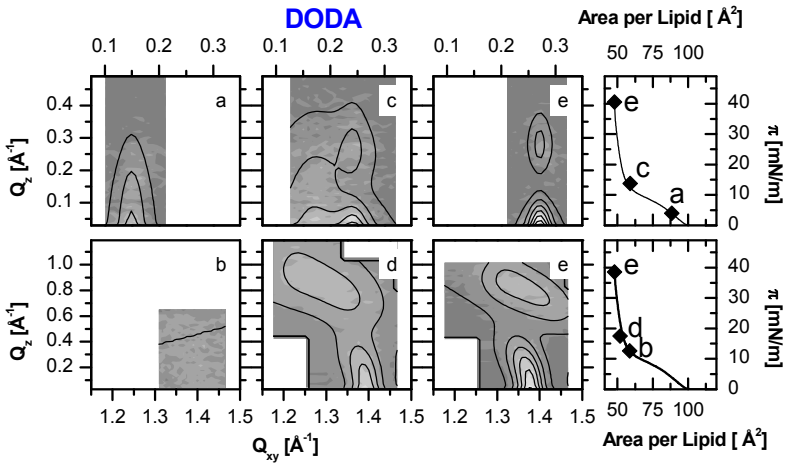

(**a**)

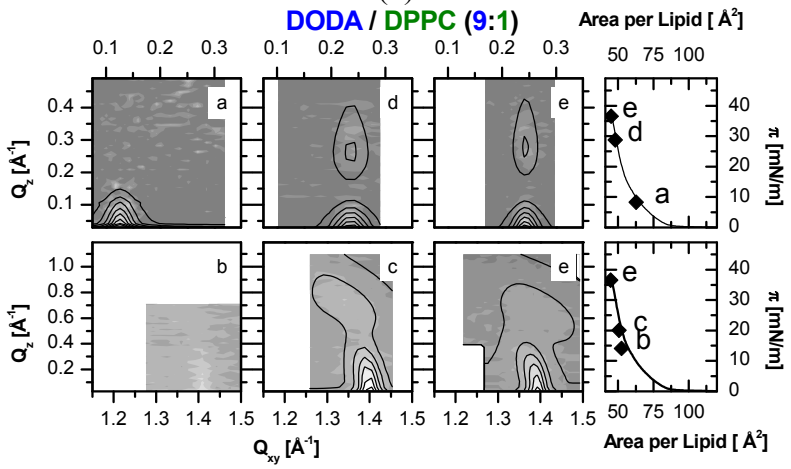

(**b**)

Figure 3. *Cont.*

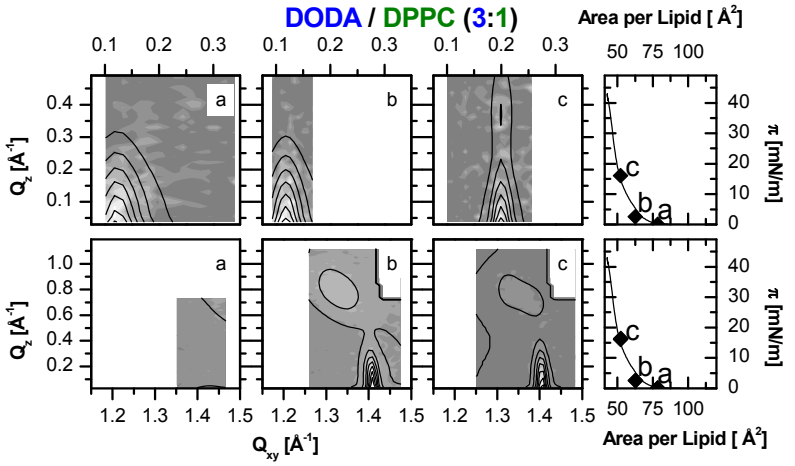

(**c**)

Figure 4 shows parameters of the alkyl tail lattice of mixed DODA/DPPC monolayers. The proportion of DODA is varied. The area per molecule A_{diffr} measured by diffraction correlates with the tilt angle t according to $A_{\mathrm{diffr}} = A_{\mathrm{tail}}/\cos(t)$ [1]. A_{tail} is the average area of the tails, measured perpendicular to the long axis. One obtains $A_{\mathrm{tail}} = 20$ Å^2. This value is very similar to the 19.8 Å^2 known from phospholipid monolayers [1].

Figure 4. The liquid condensed (LC) phase of $\mathrm{DODA}_y\mathrm{DPPC}_{1-y}$ monolayers with different proportions of DODA. The tilt angle t is shown as a function of the area from diffraction A_{diffr} (**b**) and the correlation length of the ordered alkyl chains perpendicular to the tilt direction (**a**). The shaded area on the left side is calculated according to $t = \arccos(A_{\mathrm{diffr}} / 20)$. ($T = 20$ °C, M_{w} (PSS) = 76 kDa, $c_{\mathrm{PSS}} = 0.01$ mmol/L with respect to the monomer concentration).

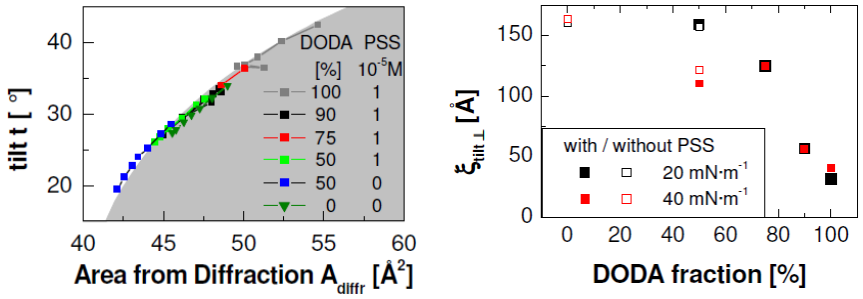

(**a**) (**b**)

Additionally, Figure 4 shows that pure DODA films have the largest tilt angles, on addition of DPPC the tilt angle decreases. The smallest tilt angle is found for 50% DPPC, without adsorbed PSS. The tilt angle of pure DPPC is again larger; it is similar to a mixture with 75%–90% DODA or 50% DODA with adsorbed PSS. A decreased tilt angle means that a monolayer can be compressed to smaller molecular areas. This effect is indeed observed in the isotherms (see Figure 1). The structure of pure DODA is a monoclinic lattice with a broad azimuth distribution [13] and a small correlation length $\xi_{\mathrm{tilt},\perp}$ perpendicular to the tilt angle (≈30 Å) [14]. Pure DPPC has an orthorhombic lattice, the

respective correlation length $\xi_{tilt,\perp}$ is larger (≈150 Å). Figure 4 shows the dependence of $\xi_{tilt,\perp}$ on the film composition. $\xi_{tilt,\perp}$ increases on decrease of the DODA proportion. When the DODA proportion is 50%, the correlation length is almost as large as for pure DPPC monolayers. The dependence of the tilt angle and of the correlation length on the monolayer composition confirms our assumption that DODA and DPPC form homogeneous mixtures.

In the next step, PSS is replaced by the statistical copolymer P–trisAA$_x$–rand–AMPS$_{1-x}$ with a reduced line charge. DODA monolayers with their large surface charge are used. Again, small-angle diffraction peaks due to aligned PE chains are observed (Figure 5). Always, these are simple peaks, without a structured rod. For the copolymer with the higher line charge, P–trisAA$_{0.1}$–rand–AMPS$_{0.9}$, peaks are observed along the whole isotherm, when the lipids are in the LE and the LC phase (see wide-angle diffraction peaks). However, for P–trisAA$_{0.5}$–rand–AMPS$_{0.5}$ with its reduced line charge, small angle peaks are observed only when DODA is in the LE phase. In the LC phase, wide angle GID peaks due to ordered alkyl tails are found, but there are no low angle peaks due to aligned PSS chains.

Figure 5. Small and wide angle GID measurements along DODA isotherms at the molecular areas indicated. The subphase contains 0.01 mmol/L P–trisAA$_x$–rand–AMPS$_{1-x}$ (with respect to the monomer concentration), T = 20 °C. The low-angle diffraction peaks are due to aligned PE chains, the wide-angle peaks measure the DODA structure. (**a**) P–TrisAA$_{0.1}$–rand–AMPS$_{0.9}$. (**b**) P–TrisAA$_{0.5}$–rand–AMPS$_{0.5}$. Always, background is subtracted and contour plots are calculated from least square fits to appropriate models.

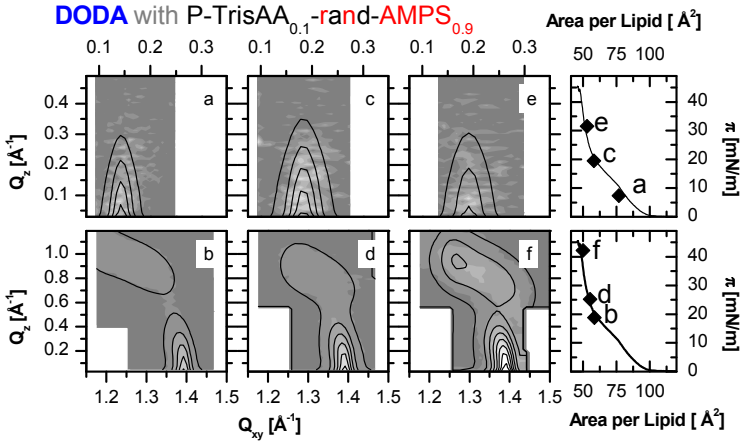

(**a**)

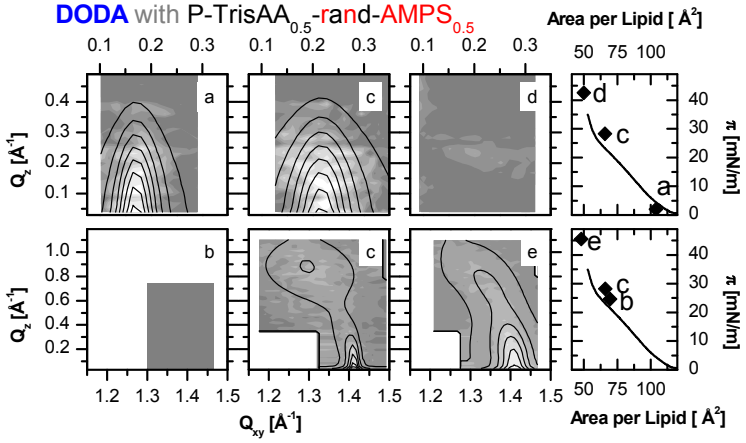

(**b**)

Quantification of polyelectrolyte coverage: In Figure 6, the interchain separation d_{PE} as deduced from the low angle GID peaks is plotted for the different systems. On monolayer compression, it decreases at most by a factor of two, provided the monolayer shows both a LE and a LC phase. Also shown is the ratio of lipid molecules to PE monomers, n_{PE}/n_{Lipid}. To get further insight into electrostatic interactions, the ratio between charged PE monomers and charged lipid molecules is given, ch_{PE}/ch_{Lipid}. For these calculations, the average molecular area A is determined from the isotherms, and multiplied if necessary with y, the mole fraction of charged lipids. Similarly, the area per monomer is determined from the monomer length multiplied by the interchain separation d_{PE} ($A_{monomer}$ = 2.5 Å d_{PE}; 2.5 Å is the monomer length of all PEs, see Scheme 2), and if appropriate by $(1 - x)$, the mole fraction of charged monomers of P–trisAA$_x$–rand–AMPS$_{1-x}$.

Figure 6. Top row: The dependence of the interchain separation d_{PE} on the molecular area A of the lipids. The left panel (**a**) shows PSS adsorbed to DODA/DPPC monolayers (composition indicated), the right panel (**b**) P–TrisAA$_x$–rand–AMPS$_{1-x}$ adsorbed to DODA. Center row: the ratio between PE monomers and lipid molecules, n_{PE}/n_{Lipid}. Bottom row: ratio of charged PE monomers to charged lipid molecules, ch_{PE}/ch_{Lipid}.

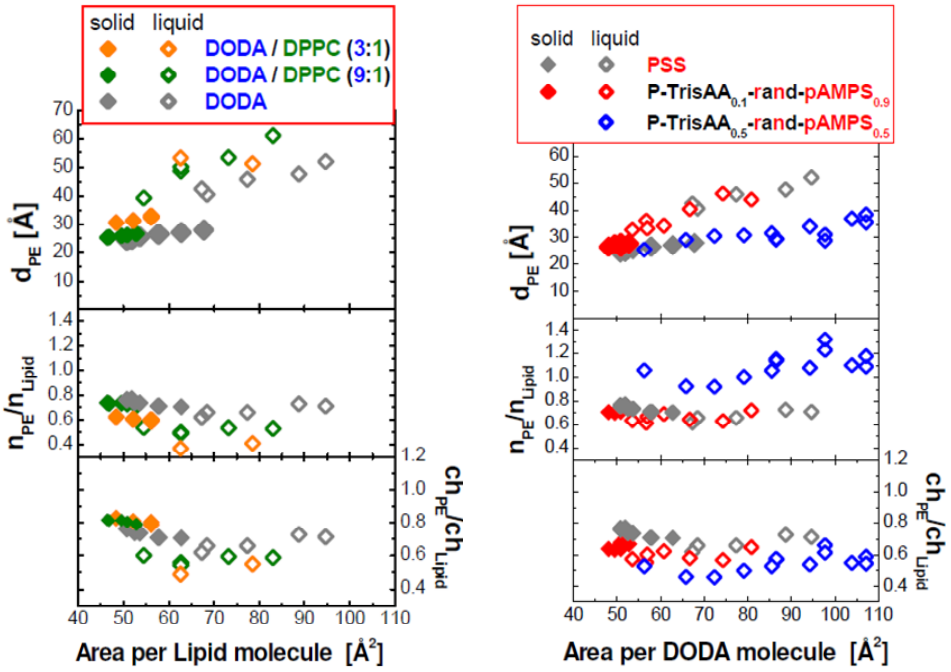

(**a**) (**b**)

For the mixed DODA/DPPC monolayers with adsorbed PSS, d_{PE} increases with decreasing surface charge. This observation is valid when the lipids are in the LC phase, in the LE phase, or the coexistence region of the LE and LC phase. A comparison of the three monolayers shows that a decrease of the fraction of the charged lipids causes a decrease in the ratio n_{PE}/n_{Lipid} (see Figure 6). However, the ratio between PSS monomers and charged lipids, ch_{PE}/ch_{Lipid}, is between 0.5 and 0.8. Expected are values below 1, reversal of the surface charge hinders the formation of the lamellar phase. ch_{PE}/ch_{Lipid} is largest for the system with the highest surface and linear charge density, DODA monolayers (see Figure 6). It is slightly larger for DODA in the LC phase (ch_{PE}/ch_{Lipid} = 0.74 and

0.67). In the LC phase, ch_{PE}/ch_{Lipid} increases to about 0.8. However, in the LE phase, ch_{PE}/ch_{Lipid} decreases with decreasing fraction of charge lipids.

Next, pure DODA monolayers with adsorbed PSS and statistical copolymer P–TrisAA$_x$–rand–AMPS$_{1-x}$, are compared (see Figure 5b). For PSS and the statistical copolymer with 90% charged monomers, d_{PE} coincides within resolution for all phases of the lipid monolayer. When 50% of the monomers are charged, d_{PE} is drastically decreased. The interchain separation is smaller, *i.e.*, the surface coverage of the PE is larger. For this PE, P–TrisAA$_{0.5}$–rand–AMPS$_{0.5}$, Bragg peaks can only be observed when the DODA monolayer is in the LE phase. n_{PE}/n_{Lipid} shows that for this copolymer with the low line charge about one monomer per lipid molecule is adsorbed. This ratio between PE monomers and lipid molecules suggests that in the LC phase the interchain separation is 20 Å or less, *i.e.*, that the polyelectrolyte chains touch each other [13]. Then, no Bragg peaks can be resolved. This makes sense if the physics of diffraction is considered. A domain of aligned PEs is ordered only in one dimension (perpendicular to the chains). To obtain a Bragg peak, the scattering center is obtained by integrating along the PE backbone. A polyelectrolyte is not a stiff rod, but it is flexible. When the positional broadening (in the direction perpendicular to the chain) approaches the distance between adjacent PE chains, no diffraction peaks form. Also, when the chains are adsorbed in a flat disordered phase, no Braggs peaks are observed.

Nevertheless, when we consider the ratio between charged monomers and lipid molecules, we get again values below 1. ch_{PE}/ch_{Lipid} depends on the phase of the lipids. When the lipid phase is unchanged, ch_{PE}/ch_{Lipid} changes little during monolayer compression (see Figure 6). Therefore, we consider the average of ch_{PE}/ch_{Lipid} for each lipid phase (see Figure 7). For each system investigated, ch_{PE}/ch_{Lipid} is larger in the LC phase than in the LE phase. When the surface charge is varied, ch_{PE}/ch_{Lipid} is fairly constant, suggesting that the adsorption is mainly due to electrostatic forces. However, with decreasing linear charge, ch_{PE}/ch_{Lipid} decreases. The neutral monomers seem to interact strongly with the DODA monolayer; other interactions besides electrostatic forces have to be considered.

Figure 7. Ratio of charged adsorbed PE monomers to charged lipid molecules ch_{PE}/ch_{Lipid} as function of the surface charge or linear charge density, respectively. Each value of ch_{PE}/ch_{Lipid} shown is the average of all GID measurements taken from the lipid phase indicated. (**a**) DODA$_y$DPPC$_{1-y}$ monolayers with adsorbed PSS. (**b**) DODA monolayers with adsorbed PE (PSS, P–TrisAA$_x$–rand–AMPS$_{1-x}$ with x = 0.9, 0.5). Symbol assignment and color code is the same as in Figure 6.

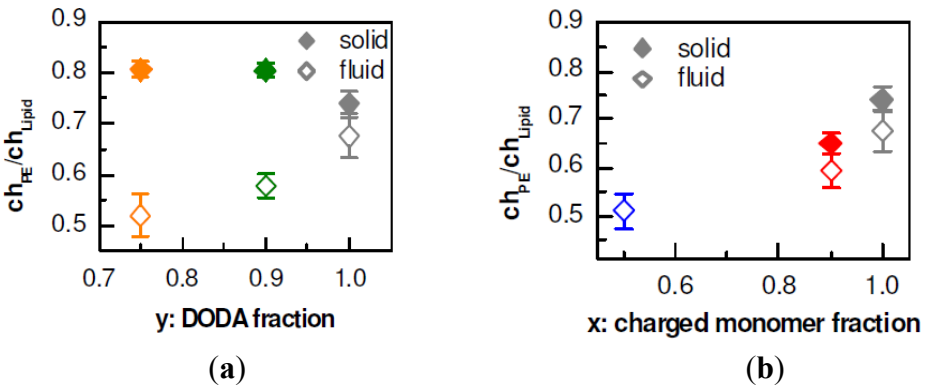

The correlation length is a measure of the extension of lateral order. Figure 8 shows ξ_{PE}, the correlation length of the domains consisting of aligned PEs. ξ_{PE} depends on the phase of the lipids. When the monolayer is compressed within a lipid phase, ξ_{PE} does not change [14]. Therefore, we consider the average of ξ_{PE} for each lipid phase (see Figure 8). The largest value (≈75 Å with lipids in LC phase) is found for the system with the largest electrostatic forces, DODA and PSS. On decrease of the surface charge density, the correlation length decreases. However, the interchain separation increases. To get an idea of the extension of the order within the two-dimensional lamellar phase, we consider the ratio ξ_{PE}/d_{PE} (see Figure 8), again the average value for each lipid phase. The largest correlation length 364 ξ_{PE} is found for PSS adsorbed to DODA in the LC phase, it corresponds to three times d_{PE}.

Figure 8. Left: $DODA_yDPPC_{1-y}$ monolayers with adsorbed PSS (76 kDa). Right: DODA monolayers with adsorbed PE (PSS, P–$TrisAA_x$–rand–$AMPS_{1-x}$ with x = 0.9, 0.5). Top: Correlation length ξ_{PE} of adsorbed PEs as function of the surface charge density or linear charge density, respectively. Bottom: Ratio between correlation length ξ_{PE} and interchain separation dPE. ξ_{PE} and ξ_{PE}/d_{PE} are the average of all GID measurements taken from the lipid phase indicated. Symbol assignment and color code is the same as Figure 6.

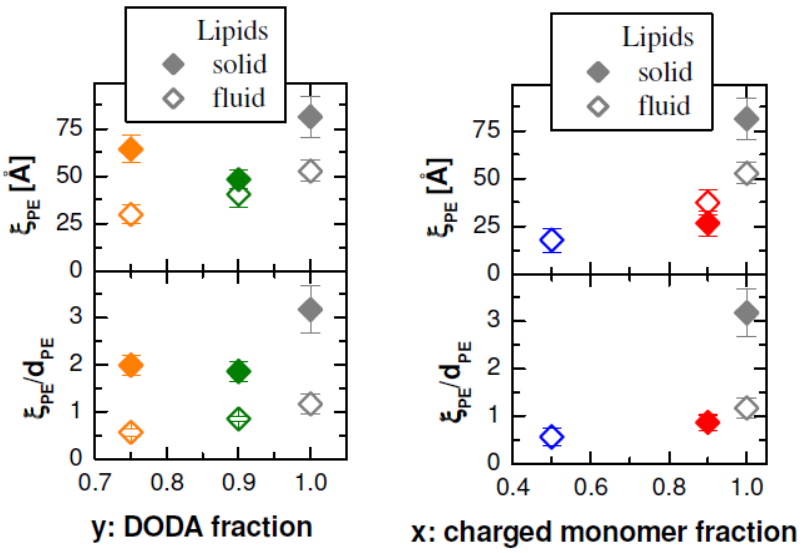

For all $DODA_yDPPC_{1-y}$ monolayers, we find a larger correlation length ξ_{PE} when PSS adsorbs to the LC phase than to the LE phase. This finding was attributed to a larger mobility of PSS adsorbed to lipids in the LE phase [12,14]. On decrease of the surface charge density, the correlation length ξ_{PE} decreases. If PSS adsorbs to lipids in the LC phase, the ratio ξ_{PE}/d_{PE} decreases from 3 to 2. However, if the lipids are in the LE phase, the decrease is more drastic, from 1.3 to 0.6. The small value of ξ_{PE}/d_{PE} suggests that on further decrease of the surface charge density PSS will adsorb no longer in the 2-D lamellar phase, but in a flatly disordered phase.

For the statistic copolymer adsorbed to DODA, the picture is more complex. Already for the strongly charged P–$TrisAA_{0.1}$–rand–$AMPS_{0.9}$, we obtain ξ_{PE}/d_{PE} = 1, independent of the lipid phase. The order of the aligned PE chains is very short-ranged. When the proportion of charged monomers is decreased (P–$TrisAA_{0.5}$–rand–$AMPS_{0.5}$), Bragg peaks due to aligned PE molecules are only found when the lipids

are in the LE phase. ξ_{PE}/d_{PE} is small, only 0.6. When the lipids are in the LC phase, d_{PE} decreases further. Now, the positional broadening of the PE chain (in the direction perpendicular to the chain) exceeds the distance between adjacent PE chains, no diffraction peaks can form. This is indeed observed.

Actually, we developed a model of the density distribution of the adsorbed PE chains beneath the lipids described in [13]. Briefly, PE chains with high electron density are embedded in water with lower electron density. The electron density ρ_{total} is the sum of a laterally homogeneous part, $\rho(z)$ (determined in X-ray reflectivity measurements) and its local deviation $\rho_{diff}(x,y,z)$, with $\int \mathrm{d}x\mathrm{d}y\rho_{diff}(x,y,z)=0$. The molecular form factor is given by the Fourier transformation, $\left|F_{\mathrm{mol}}(Q_z)\right|^2=\left|\int\int\int \mathrm{d}x\mathrm{d}y\mathrm{d}z\cdot\rho_{\mathrm{diff}}(x,y,z)\cdot\exp(iQ_x x+iQ_y y+iQ_z z\right|^2$. When a Bragg peak in Q_{xy}–direction is observed, then one obtains $Q_{xy}=Q_{\mathrm{peak}}=\frac{2\pi}{d_{\mathrm{PE}}}$. The lateral structure exhibits a periodicity of width d_{PE}, consisting of a chain with a diameter d_{chain} and electron density ρ_{PE} embedded in water (width $d_{PE} - d_{chain}$, electron density ρ_{H2O}). Focusing on the in-plane integration at the peak position, one has $\tilde{\rho}_{\mathrm{diff}}(z)=\int\int \mathrm{d}x\mathrm{d}y\cdot\rho_{\mathrm{diff}}(x,y,z)\cdot\exp(iQ_x x+iQ_y y)$. Performing the integration at Q_{peak} yields $\tilde{\rho}_{\mathrm{diff}}(z)=\frac{d_{\mathrm{PE}}(\rho_{\mathrm{PE}}-\rho_{\mathrm{H_2O}})}{2\pi}\sin(\frac{\pi\cdot d_{\mathrm{chain}}}{d_{\mathrm{PE}}})$. For P–TrisAA$_{0.1}$–rand–AMPS$_{0.9}$, one obtains ρ_{PE} = 0.372 e$^-$/Å^3, which decreases for P–TrisAA$_{0.5}$–rand–AMPS$_{0.5}$ to 0.356 e$^-$/Å^3. When the lipids are in the fluid phase, one obtains for $\tilde{\rho}_{\mathrm{diff}}(z)$ the values 0.202 and 0.100 e$^-$/Å^2, respectively. In the gel phase, d_{PE} is decreased, and so is $\tilde{\rho}_{\mathrm{diff}}(z)$, down to 0.165 and 0.031 e$^-$/Å^2, respectively. The latter number is an estimate, since below the lipids in the gel phase, no peak of P–TrisAA$_{0.5}$–rand–AMPS$_{0.5}$ is observed (see Figure 5); we assumed d_{PE} = 15 Å. Note that $\tilde{\rho}_{\mathrm{diff}}(z)$ is low for two reasons: (a) P–TrisAA$_{0.5}$–rand–AMPS$_{0.5}$ has an electron density more similar to water than the random copolymer with the larger linear charge density and (b) d_{PE} approaches the diameter of P–TrisAA$_{0.5}$–rand–AMPS$_{0.5}$ (15 and 12 Å, respectively).

The description of the adsorbed PEs helps to understand the transition enthalpy ΔH shown in Figure 2. The temperature dependence of ΔH is decreased when the random copolymer has a larger proportion of neutral monomers. A reduced transition enthalpy ΔH with weak temperature dependence is found when the lipids in the LE phase are partly immobilized by network formation [14]. We suggest that the neutral monomers TrisAA bind strongly to the lipids, reduce the mobility of DODA molecules in the LE phase, and thus influence the phase transition. While this work focuses on electrostatic interactions, the changed isotherm due to weakly charged trisAA$_{0.5}$–rand–AMPS$_{0.5}$ highlights the importance of not-electrostatic interactions between polyelectrolytes and model membranes.

4. Conclusions

A combination of thermodynamic analysis and Grazing Incidence X-ray Diffraction (GID) is used to investigate the adsorption of PEs to oppositely charged lipid monolayers. The shed some light on the role of electrostatic forces in PE adsorption, lipid monolayers of different composition (mixtures of DPPC and DODA) and PEs with different linear charge density (the statistic copolymer P–TrisAA$_x$–rand–AMPS$_{1-x}$ with x = 0.5, 0.9) are used. The PE concentration in solution is 0.01 mmol/L (in monomer units), to make PE adsorption in the 2-dimensional lamellar phase possible. Grazing Incidence X-ray diffraction

allows determining the interchain separation during the monolayer compression, and thus to quantify the effects of surface and linear charge density (see Scheme 3).

In most cases we find the 2-dimensional lamellar phase. The ratio of charged PE monomers to charged lipid molecules, ch_{PE}/ch_{Lipid}, is always smaller one. The adsorbed PEs decrease but do not inverse the surface charge of the monolayer, as predicted theoretically [15,16]. However, for all systems investigated, ch_{PE}/ch_{Lipid} is larger when the lipids are in the LC phase. ch_{PE}/ch_{Lipid} decreases by 30% or less, when the line charge density or the surface charge density is decreased and the lipids are in the LE phase. The ratio of charged monomers to lipid molecules, ch_{PE}/ch_{Lipid} depends on the phase of the lipids, it is not changed during compression of the respective lipid phase. This observation suggests that the PE/lipid interaction depends weakly on the lipid phase. ch_{PE}/ch_{Lipid} is largest for DODA/PSS, the system with the highest surface charge density and the highest linear charge density.

Scheme 3. (**a**) Side view of a mixed lipid monolayer with decreased surface charge density. Shown is the view along the PE chain (left) and perpendicular to the PE chain (right). Few PE chains are adsorbed. (**b**) A highly charged monolayer with an adsorbed PE layer with decreased linear charge density. Both negatively charged and neutral monomers are adsorbed.

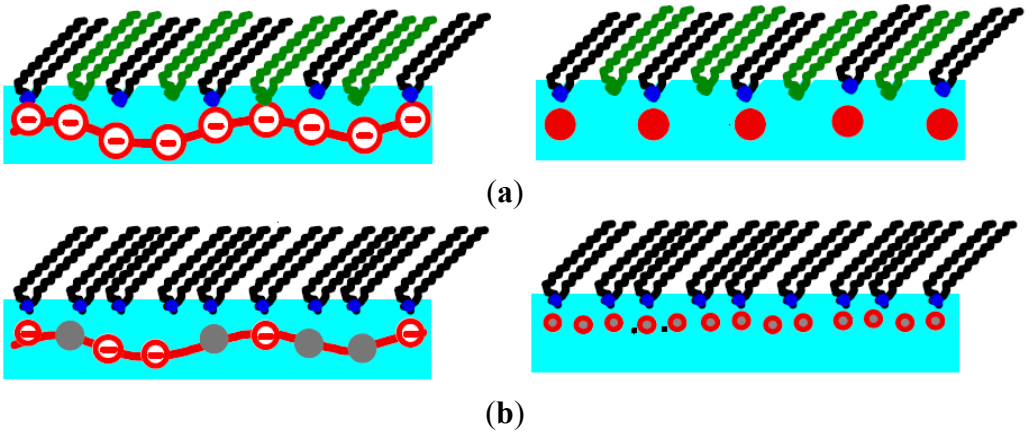

(**a**)

(**b**)

ch_{PE}/ch_{Lipid} varies, by 30%. For all $DODA_yDPPC_{1-y}$ monolayers, ch_{PE}/ch_{Lipid} is larger when the lipids are in the LC phase. Nevertheless, some features are obvious: On decreasing the surface charge density, less PE adsorbs, to keep ch_{PE}/ch_{Lipid} more or less constant. Conversely, on decreasing the line charge, more PE adsorbs, and ch_{PE}/ch_{Lipid} shows a small decrease. Therefore, mainly electrostatic forces determine how much PE adsorbs in the two-dimensional lamellar phase. Actually, with decreasing surface charge or linear charge density, the extension of the lamellar order decreases. The smallest values of the correlation length observed are about half a chain separation.

Concluding, the combination of structural and thermodynamic data is a very powerful approach. Grazing Incidence Diffraction allows determining the surface coverage and especially the phase of the adsorbed polyelectrolyte. Thus, insight into the polyelectrolyte-monolayer interaction and the relative importance of electrostatic interactions is possible.

Acknowledgments

We thank Hamburger Synchrotron laboratory (HASYLAB) at Deutsches Elektronen-Synchrotron (DESY), Hamburg, Germany for beam time and for providing all necessary facilities. Discussions with Burkhard Dünweg were helpful. Financial support of the Deutsche Forschungsgemeinschaft (DFG) (He 1616/14-1) is appreciated.

Author Contributions

This collaboration between Potsdam and Greifswald University has been directed at understanding and modifying the phases of PEs at interfaces. Thomas Ortmann is a doctoral student, supervised by Christiane A. Helm. He is responsible for the characterization of PEs adsorbed to lipid monolayers. Heiko Ahrens, Andreas Gröning and Frank Lawrenz helped with the experiments at the synchrotron; Heiko Ahrens was also instrumental in the analysis of the diffraction peaks. Sven Milewski was a Bachelor student who worked on lipid mixtures. Sebastian Garnier and André Laschewsky designed, synthesized and characterized the polyelectrolyte random copolymers of varying charge at Universität Potsdam.

Conflicts of Interest

The authors declare no conflict of interest.

References

1. Kaganer, V.M.; Möhwald, H.; Dutta, P. Structure and phase transitions in Langmuir monolayers. *Rev. Mod. Phys.* **1999**, *71*, 779–819.
2. Möhwald, H. Phospholipid and phospholipid protein monolayers at the air/water interface. *Annu. Rev. Phys. Chem.* **1990**, *41*, 441–476.
3. McConnell, H.M. Structures and transitions in lipid monolayers at the air-water-interface. *Annu. Rev. Phys. Chem.* **1991**, *42*, 171–195.
4. Dahmen-Levison, U.; Brezesinski, G.; Möhwald, H. Specific adsorption of PLA_2 at monolayers. *Thin Solid Films* **1998**, *327–329*, 616–620.
5. Brezesinski, G.; Möhwald, H. Langmuir monolayers to study interactions at model membrane surfaces. *Adv. Colloid Interface Sci.* **2003**, *100*, 563–584.
6. Holten-Andersen, N.; Michael Henderson, J.; Walther, F.J.; Waring, A.J.; Ruchala, P.; Notter, R.H.; Lee, K.Y.C. KL_4 peptide induces reversible collapse structures on multiple length scales in model lung surfactant. *Biophys. J.* **2011**, *101*, 2957–2965.
7. Paiva, D.; Brezesinski, G.; Pereira, M.D.; Rocha, S. Langmuir monolayers of monocationic lipid mixed with cholesterol or fluorocholesterol: DNA adsorption studies. *Langmuir* **2013**, *29*, 1920–1925.
8. Möhwald, H.; Menzel, H.; Helm, C.A.; Stamm, M. Lipid polyampholyte monolayers to study polyelectrolyte interactions and structure at surfaces. *Adv. Polym. Sci.* **2004**, *161*, 151–175.
9. Berndt, P.; Kurihara, K.; Kunitake, T. Adsorption of poly(styrenesulfonate) onto an ammonium monolayer on mica: A surface forces study. *Langmuir* **1992**, *8*, 2486–2490.
10. Lowack, K.; Helm, C.A. Molecular mechanisms controlling the self-assembly process of polyelectrolyte multilayers. *Macromolecules* **1998**, *31*, 823–833.

11. Szilagyi, I.; Trefalt, G.; Tiraferri, A.; Maroni, P.; Borkovec, M. Polyelectrolyte adsorption, interparticle forces, and colloidal aggregation. *Soft Matter* **2014**, *10*, 2479–2502.
12. Gromer, A.; Rawiso, M.; Maaloum, M. Visualization of hydrophobic polyelectrolytes using atomic force microscopy in solution. *Langmuir* **2008**, *24*, 8950–8953.
13. Günther, J.U.; Ahrens, H.; Helm, C.A. Two-dimensional lamellar phase of poly(styrene sulfonate) adsorbed onto an oppositely charged lipid monolayer. *Langmuir* **2009**, *25*, 1500–1508.
14. Ortmann, T.; Ahrens, H.; Lawrenz, F.; Gröning, A.; Nestler, P.; Günther, J.-U.; Helm, C.A. Lipid monolayers and adsorbed polyelectrolytes with different degree of polymerization. *Langmuir* **2014**, *30*, 6768–6779.
15. Netz, R.R.; Joanny, J.-F. Adsorption of semiflexible polyelectrolytes on charged planar surfaces: Charge compensation, charge reversal, and multilayer formation. *Macromolecules* **1999**, *32*, 9012–9025.
16. Netz, R.R.; Andelman, D. Neutral and charged polymers at interfaces. *Phys. Rep.* **2003**, *380*, 1–95.
17. Pavinatto, F.J.; Caseli, L.; Pavinatto, A.; dos Santos, D.S., Jr.; Nobre, T.M.; Zaniquelli, M.E.D.; Silva, H.S.; Miranda, P.B.; de Oliveira, O.N., Jr. Probing chitosan and phospholipid interactions using Langmuir and Langmuir-Blodgett films as cell membrane models. *Langmuir* **2007**, *23*, 7666–7671.
18. Kiss, É.; Heine, E.T.; Hill, K.; He, Y.C.; Keusgen, N.; Pénzes, C.B.; Schnöller, D.; Gyulai, G.; Mendrek, A.; Keul, H.; *et al.* Membrane affinity and antibacterial properties of cationic polyelectrolytes with different hydrophobicity. *Macromol. Biosci.* **2012**, *12*, 1181–1189.
19. Engelking, J.; Menzel, H. Adsorption of anionic polyelectrolytes to dioctadecyldimethylammonium bromide monolayers. *Eur. Phys. J. E* **2000**, *5*, 87–96.
20. Engelking, J.; Ulbrich, D.; Menzel, H. Piezochromic effect and orientational order in monolayers and multilayers of poly(*p*-phenylenesulfonate)-dioctadecyldimethylammonium bromid complexes. *Macromolecules* **2000**, *33*, 9026–9033.
21. Messina, R. Electrostatics in soft matter. *J. Phys. Condens. Matter.* **2009**, *21*, doi:10.1088/0953-8984/21/11/113102.
22. Helm, C.A.; Laxhuber, L.; Lösche, M.; Möhwald, H. Electrostatic interactions in phospholipid membranes: Influence of monovalent ions. *Colloid Polym. Sci.* **1986**, *264*, 46–55.
23. Schönhoff, M. Layered polyelectrolyte complexes: Physics of formation and molecular properties. *J. Phys. Condens. Matter* 2003, *15*, R1781–R1808.
24. Ahrens, H.; Baltes, H.; Schmitt, J.; Möhwald, H.; Helm, C.A. Polyelectrolyte adsorption onto liquid surfaces. *Macromolecules* **2001**, *34*, 4504–4512.
25. Delorme, N.; Dubois, M.; Garnier, S.; Laschewsky, A.; Weinkamer, R.; Zemb, T.; Fery, A. Surface immobilization and mechanical properties of catanionic hollow faceted polyhedrons. *J. Phys. Chem. B* **2006**, *110*, 1752–1758.
26. Kjaer, K.; Als-Nielsen, J.; Helm, C.A.; Laxhuber, L.A.; Möhwald, H. Ordering in lipid monolayers studied by synchrotron X-Ray diffraction and fluorescence microscopy. *Phys. Rev. Lett.* **1987**, *58*, 2224–2227.
27. Ahrens, H.; Papastavrou, G.; Schmidt, M.; Helm, C.A. Synchrotron X-ray diffraction and reflection studies of a polymacromonomer monolayer at the air-water interface: Transition from straight aligned molecules to homogeneous layer. *J. Phys. Chem. B* **2004**, *108*, 16870–16876.

28. Kenn, R.M.; Kjaer, K.; Möhwald, H. Non-rotator phases in phospholipid monolayers? *Colloids Surf. A* **1996**, *117*, 171–181.
29. Helm, C.A.; Möhwald, H.; Kjaer, K.; Als-Nielsen, J. Phospholipid monolayer density distribution perpendicular to the water surface. A synchrotron X-ray reflection study. *Europhys. Lett.* **1987**, *4*, 697–703.